

Report

Rapid De Novo Centromere Formation Occurs Independently of Heterochromatin Protein 1 in *C. elegans* Embryos

Karen W.Y. Yuen,^{1,3} Kentaro Nabeshima,² Karen Oegema,¹ and Arshad Desai^{1,*}

¹Ludwig Institute for Cancer Research and Department of Cellular and Molecular Medicine, University of California, San Diego, La Jolla, CA 92037, USA

²Department of Cell and Developmental Biology, University of Michigan Medical School, Ann Arbor, MI 48109-2200, USA

Summary

DNA injected into the *Caenorhabditis elegans* germline forms extrachromosomal arrays that segregate during cell division [1, 2]. The mechanisms underlying array formation and segregation are not known. Here, we show that extrachromosomal arrays form de novo centromeres at high frequency, providing unique access to a process that occurs with extremely low frequency in other systems [3–8]. De novo centromerized arrays recruit centromeric chromatin and kinetochore proteins and autonomously segregate on the spindle. Live imaging following DNA injection revealed that arrays form after oocyte fertilization via homologous recombination and nonhomologous end-joining. Individual arrays gradually transition from passive inheritance to active segregation during the early embryonic divisions. The heterochromatin protein 1 (HP1) family proteins HPL-1 and HPL-2 are dispensable for de novo centromerization even though arrays become strongly enriched for the heterochromatin-associated H3K9me3 modification over time. Partial inhibition of HP1 family proteins accelerates the acquisition of segregation competence. In addition to reporting the first direct visualization of new centromere formation in living cells, these findings reveal that naked DNA rapidly builds de novo centromeres in *C. elegans* embryos in an HP1-independent manner and suggest that, rather than being a prerequisite, HP1-dependent heterochromatin antagonizes de novo centromerization.

Results and Discussion

Extrachromosomal Arrays in *C. elegans* Form Centromeres and Segregate Autonomously

DNA injected into the *C. elegans* germline forms extrachromosomal arrays that segregate during cell division and can be transmitted across generations [1, 2]. To determine whether extrachromosomal arrays segregate using centromeres [9, 10] or employ an alternative mechanism, such as the “hitchhiking” of double-minute chromosomes and certain viral replicons [11], we constructed arrays by injecting a mixture of two plasmids (Figure 1A). The first plasmid (p64xLacO) included 64 Lac operator repeats, allowing array visualization using Lac repressor (LacI). The second plasmid (pRF4) encoded

the dominant mutant *rol-6(su1006)*, which makes worms roll in a circular pattern (Roller phenotype) [1]. Three independent strains containing propagating arrays (each passed for more than five generations) were generated, and arrays were visualized in fixed embryos using recombinant LacI. Typically, one or two copies of each array were observed per mitotic nucleus (Figure 1C). Arrays were transmitted with >95% fidelity during embryonic cell divisions. Array inheritance across generations, which requires transmission through the mitotic proliferation and meiotic segregation events that generate the gametes [12, 13], occurred at a frequency of 20%–50%. Array size was ~1 Mb based on DAPI staining using the endogenous chromosomes as standards (data not shown). Arrays lacked extended telomeric repeats, suggesting that they either are circular or have unstable ends (see Figure S1A available online).

To determine whether arrays form centromeres, we performed immunofluorescence to localize conserved centromere/kinetochore proteins (Figure 1B; [9, 10]). The centromeric histone CeCENP-A and its conserved assembly factor KNL-2 [14] localized on opposing faces of segregating arrays in a pattern similar to that on endogenous chromosomes (Figure 1C). The microtubule-binding kinetochore protein NDC-80 and the checkpoint kinase BUB-1 also localized in a similar pattern (Figure 1C), as did CENP-C and KNL-1 (Figure S1B). We conclude that arrays build centromeres for segregation, rather than employing a hitchhiking mechanism. Consistent with this, array congression independent of endogenous chromosomes could be observed on the spindle (Figure 1D). Thus, extrachromosomal arrays formed by DNA injection into the *C. elegans* germline are de novo centromerized and align and segregate autonomously on the mitotic spindle.

Extrachromosomal Arrays Form after Fertilization

By scoring for the Roller phenotype (Figure S2A), we found that injected worms produced array-containing embryos for 24 hr beginning ~4 hr after injection, which was when the first oocytes containing injected DNA were fertilized (Figure S2B). To directly visualize array formation, we imaged the gonad, oocytes, and embryos of worms expressing GFP::LacI and mCherry::H2b ~4–8 hr after injection of p64xLacO (Figure 2A). Uninjected worms contained diffuse nuclear GFP::LacI in the meiotic nuclei of the gonad, in oocytes, and in embryos (Figure 2A). In injected worms, the GFP::LacI signal in gonad nuclei and in oocytes was similar to that in uninjected worms, whereas fertilized embryos contained GFP::LacI foci that resembled stable arrays. When embryos with transmitting arrays became adults, GFP::LacI foci were detected in the meiotic and oocyte nuclei in their gonads, as well as in their embryos (Figure 2A), demonstrating that GFP::LacI is able to bind to LacO sequences in these tissues. Because only p64xLacO was injected, array formation and transmission to progeny does not require endogenous *C. elegans* DNA (see also [2]).

The above results suggested that extrachromosomal arrays are formed after oocyte fertilization rather than in the gonad where the DNA is injected. To confirm this, we imaged embryos produced by injected worms starting around oocyte

³Present address: School of Biological Sciences, Kadoorie Biological Sciences Building, The University of Hong Kong, Pok Fu Lam Road, Hong Kong

*Correspondence: abdesai@ucsd.edu

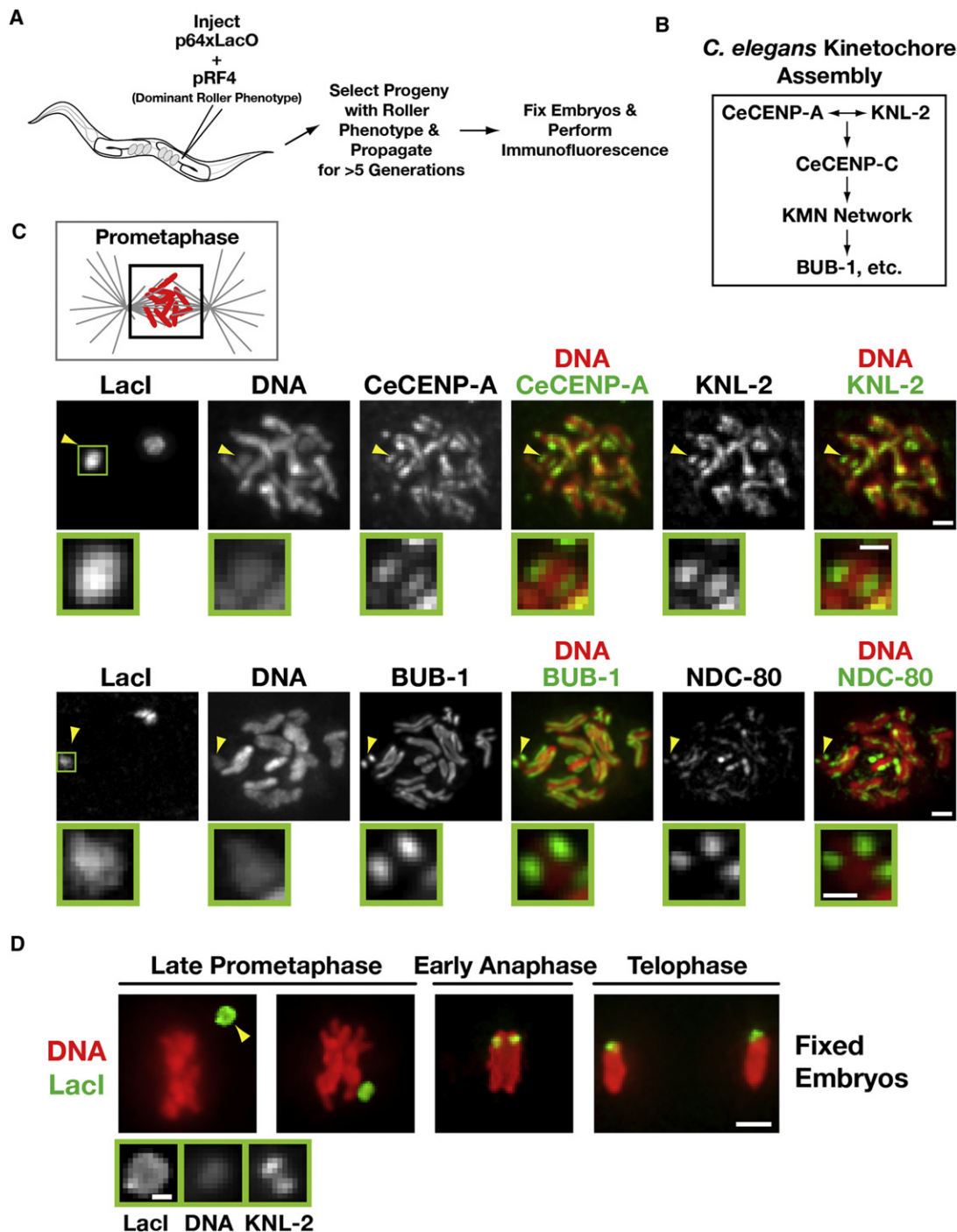


Figure 1. Kinetochore Are Present on Extrachromosomal Arrays that Have Been Propagated for Multiple Generations

(A) Schematic of experimental strategy to analyze array structure by immunofluorescence.

(B) Simplified hierarchy of *C. elegans* kinetochore assembly. The KMN network comprises KNL-1, the MIS-12 complex, and the NDC-80 complex.

(C) Chromatin-associated inner kinetochore components CeCENP-A and KNL-2 (top row) and the microtubule-binding outer kinetochore protein NDC-80 and the spindle checkpoint kinase BUB-1 (bottom row) localize to opposing faces of LacO-containing extrachromosomal arrays during prometaphase. Arrowheads point to the array; the boxed region is magnified below. Scale bar represents 1 μm (0.5 μm for magnified regions).

(D) Immunofluorescence of the LacO-containing extrachromosomal array (LacI) and DAPI staining during late prometaphase, early anaphase, and telophase in embryos. A higher-magnification view of the array (arrowhead) with KNL-2 staining is shown on the bottom. Scale bar represents 2 μm (0.5 μm for magnified regions).

meiosis II, which occurs ~ 20 min after fertilization [15]; at this stage, GFP::LacI foci were not yet visible (Figure 2B). Discrete GFP::LacI foci began to appear in the cytoplasm around

prophase of the first mitotic division (Figure 2B). These foci contained mCherry::H2b, suggesting that they are chromatinized. Numerous foci were detected per one-cell embryo

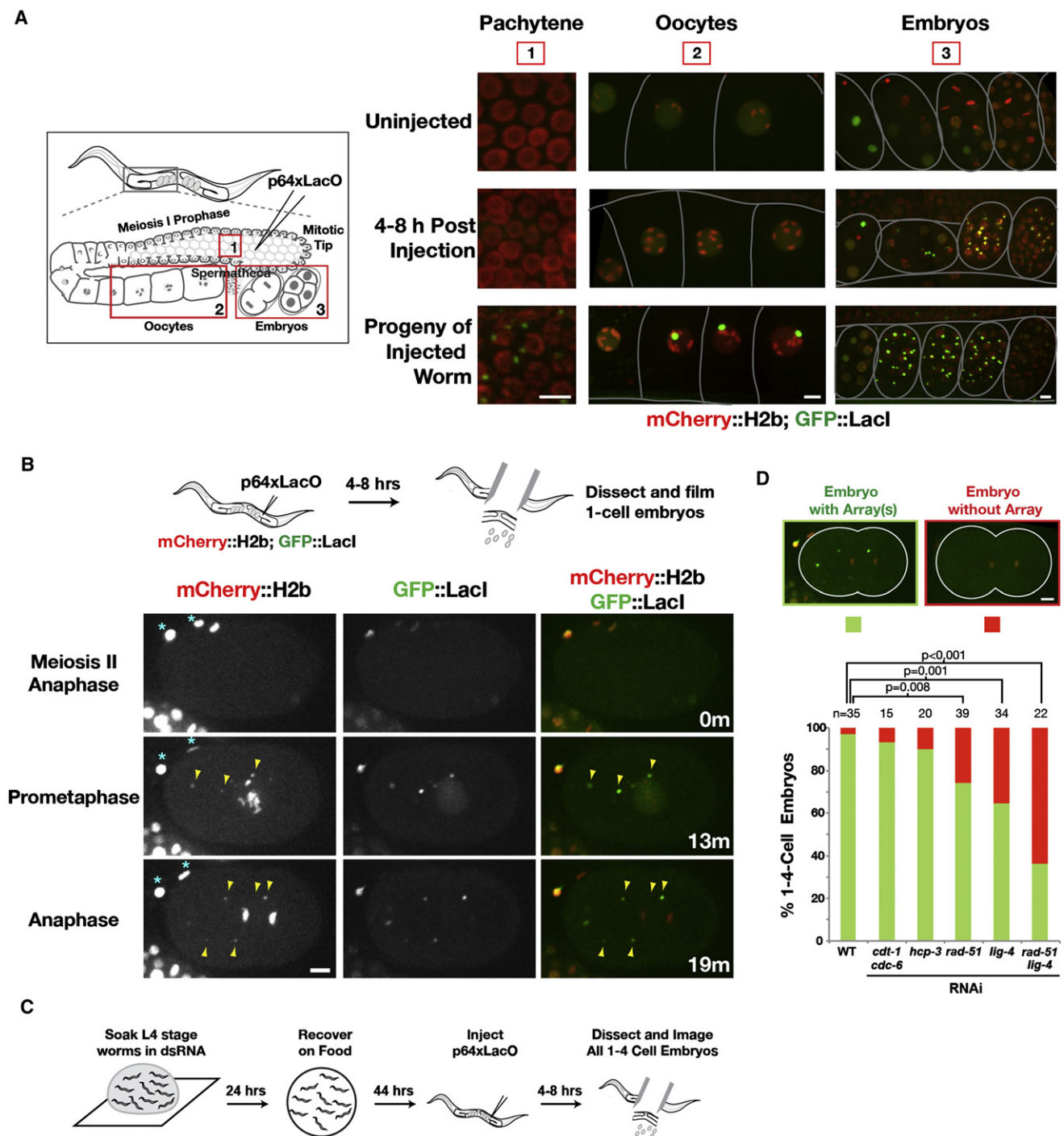


Figure 2. Timing of Extrachromosomal Array Formation

(A) Direct imaging after injection of p64xLacO into the germline of a strain expressing mCherry::H2b and GFP::LacI. Worms were anesthetized prior to imaging. The *C. elegans* germline is a syncytium comprised primarily of nuclei in meiosis I prophase; after the turn, individual nuclear compartments expand and pinch off from the syncytium to form oocytes. Fertilization by sperm stored in the spermatheca generates embryos that are stored in the uterus and eventually released into the environment. Three different regions are shown: (1) meiotic pachytene nuclei in the gonadal syncytium, (2) oocytes, and (3) embryos in the uterus. Imaging was performed on uninjected, postinjected, and progeny of injected worms, as indicated. Scale bars represent 5 μ m.

(B) Time-lapse images of a recently fertilized embryo, dissected 4–8 hr after p64xLacO injection, showing the appearance of GFP::LacI foci that also contain mCherry::H2b (arrowheads) after anaphase of meiosis II. Asterisks mark the polar bodies. Time (in minutes) relative to anaphase of meiosis II is shown. Scale bars represent 5 μ m.

(C) Schematic of the experimental approach used to analyze requirements for array formation.

(D) The bar graph shows the percentage of one- to four-cell embryos with or without arrays in the indicated conditions. Representative images of a one-cell embryo with or without an array (or arrays) are shown on top. The number of embryos (n) analyzed for each condition is indicated. p values for the indicated comparisons were obtained using a one-tailed Z test. Scale bars represent 5 μ m.

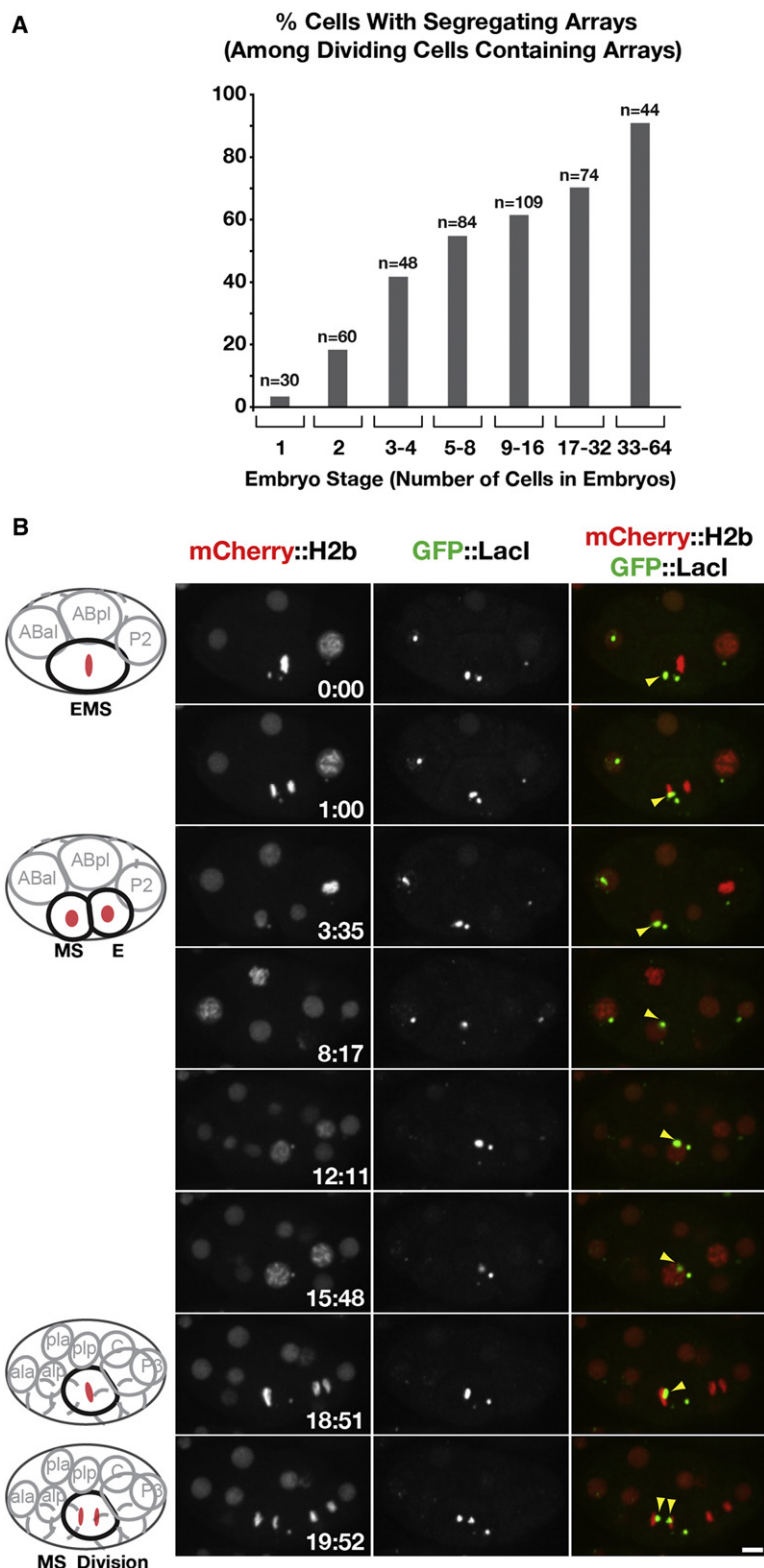


Figure 3. Extrachromosomal Arrays Acquire Segregation Competency during Early Embryonic Divisions

(A) Percentage of cells with a segregating array among all cells that contained arrays and underwent mitosis during the imaging period; x axis indicates the embryo stage. The number of cells (n) analyzed at each stage is indicated.

(B) Time-lapse images following an array that failed to segregate in the EMS cell (the precursor cell for endoderm and mesoderm in a six-cell-stage embryo) but 19 min later segregated in the daughter MS cell (the mesoderm precursor cell in a twelve-cell-stage embryo). See also [Figure S3C](#). Scale bar represents 5 μ m.

fertilization, but the ability to segregate is not acquired coincident with their formation.

To delineate the processes that contribute to array formation, we used RNA interference (RNAi) to inhibit replication initiation (CDT-1 and CDC-6), centromeric chromatin assembly (CeCENP-A/HCP-3), homologous recombination (RAD-51), and nonhomologous end-joining (LIG-4) ([Figure 2C](#)). Inhibiting replication or centromeric chromatin assembly had no effect ([Figure 2D](#); [Figures S2E](#) and [S2F](#)). In contrast, inhibiting homologous recombination or nonhomologous end-joining reduced array formation, consistent with prior analysis of array structure [2]; an additive effect was seen when both pathways were inhibited ([Figure 2D](#)). These results indicate that homologous recombination and nonhomologous end-joining concatemerize injected DNA in the cytoplasm of the one-cell embryo to form arrays. Why array formation occurs after fertilization and not in the germline where the DNA is injected is currently unclear; this timing may reflect a need for the injected DNA to access components restricted to the nuclear compartment.

Extrachromosomal Arrays Acquire Segregation Competency over Multiple Cell Cycles

Arrays selected over multiple generations show robust segregation in one-cell and later-stage embryos ([Figure 1](#)). In contrast, from 30 one-cell embryos imaged 4–8 hr after injection (total of ~100 arrays), only one array appeared to segregate ([Figure 2B](#); [Figure 3A](#); [Figure S3A](#)). These results suggest that arrays must mature to segregate. Consistent with this idea, a higher percentage of cells in later-stage embryos contained a segregation-competent array as compared to cells in early embryos ([Figure 3A](#); [Figure S3A](#)).

By following individual arrays over multiple cell cycles, we observed six examples of arrays acquiring segregation competence. In each example, the newly formed array initially failed to segregate, passively remaining in one of the two daughter cells during each division, and was then observed to align at the metaphase plate and segregate ([Figure 3B](#)). Once segregation competency was acquired, arrays continued to segregate in subsequent divisions ([Figure S3C](#)). One possibility is that nuclear access by the cytoplasmically formed arrays is required to establish segregation

(range 1–10, average 3; [Figures S2C](#) and [S2D](#)); comparison with two-cell and four-cell embryos suggested that foci formation occurred primarily during the first division ([Figures S2C](#) and [S2D](#)). Newly assembled foci did not align and segregate on the spindle. Thus, array formation occurs rapidly after

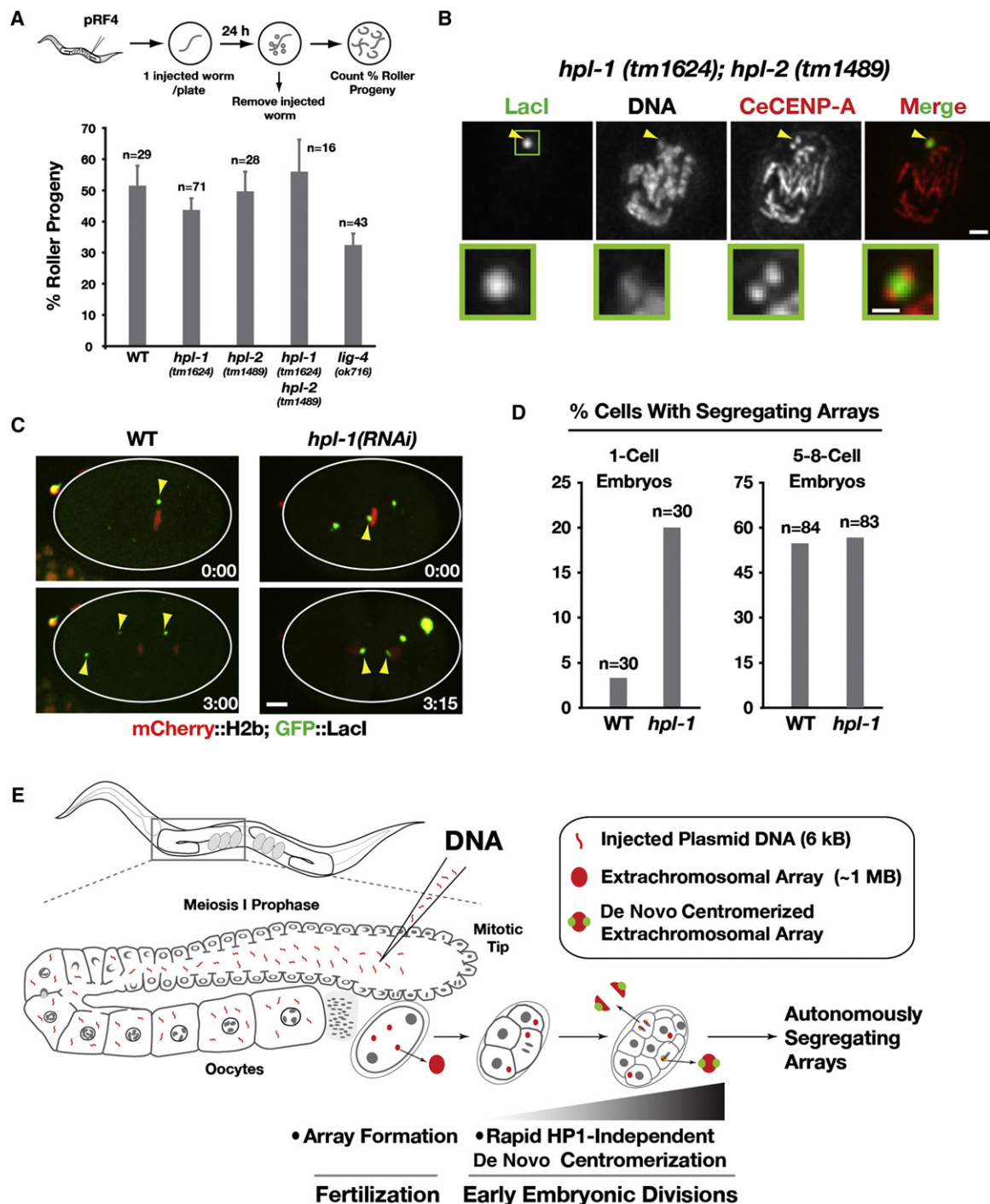


Figure 4. Heterochromatin Protein 1 Mutants, *hpl-1 hpl-2*, Do Not Affect Array Formation or De Novo Centromerization

(A) Bar graph showing the percentage of Roller progeny produced during the first 24 hr following injection of pRF4 in wild-type, *hpl-1(tm1624)*, *hpl-2(tm1489)*, *hpl-1(tm1624); hpl-2(tm1489)*, and *lig-4(ok716)* mutants. The number of worms analyzed in each condition (n) is indicated. Error bar represents 95% confidence interval for the mean.

(B) CeCENP-A localizes to opposing faces of LacO-containing extrachromosomal arrays that have been generated and propagated in the *hpl-1(tm1624); hpl-2(tm1489)* double mutant. Arrowheads point to the array; the boxed region is magnified below. Scale bar represents 1 μ m (0.5 μ m for magnified regions).

(C) Examples of one-cell embryos in wild-type and *hpl-1(RNAi)* mutants dissected and imaged 4–8 hr after p64xLacO injection. *hpl-1* RNAi was performed as in Figure 3B, except that worms were recovered for 20 hr prior to p64xLacO injection. The wild-type embryo image is the same as in Figure 2B. Scale bar represents 5 μ m.

(D) Bar graph showing the percentage of cells with a segregating array in wild-type and *hpl-1*-inhibited (using either the mutant or RNAi) embryos at the one-cell stage and at the five- to eight-cell stage. The number of cells analyzed at each stage (n) is indicated. Note that the y axis is modified to facilitate comparison of the two conditions at the two different embryo stages.

(E) Model summarizing the key findings. Array formation occurs immediately after fertilization, but array centromerization occurs over a longer timescale. HP1 family proteins are dispensable for both array formation and centromerization.

competency. Consistent with this idea, perturbing nuclear envelope disassembly in the early embryonic divisions slowed the acquisition of segregation competence (Figures S3D–S3F). Although we attempted to directly visualize centromere/kinetochore assembly, we were unable to directly correlate array maturation with the loading of centromere/kinetochore proteins as a result of close proximity of segregating arrays to endogenous chromosomes and limitations in imaging centromere/kinetochore proteins in living cells (data not shown).

Cumulatively, our results establish that array maturation lags behind array formation likely as a result of the kinetics of de novo centromerization, which may require nuclear access.

Inhibition of Heterochromatin Protein 1 Homologs, HPL-1 and HPL-2, Does Not Prevent De Novo Centromerization of Arrays

Previous work has led to conflicting views on the relationship between heterochromatin and de novo centromere formation. Studies in fission yeast and *Drosophila* have indicated that new centromere formation requires heterochromatin or a heterochromatin/euchromatin boundary [3, 4, 16–18]. By contrast, studies in mammalian cells have shown that neocentromeres can lack substantial associated heterochromatin domains [19, 20] and have suggested that heterochromatin assembly antagonizes de novo centromerization [21–23]. We therefore used extrachromosomal arrays in *C. elegans* to investigate the relationship between heterochromatin and de novo centromerization. Single-deletion mutations in the genes encoding the two HP1 family proteins HPL-1 [*hpl-1(tm1624)*] and HPL-2 [*hpl-2(tm1489)*] are viable, although both mutants exhibit a reduced brood size [24, 25]. The percentage of progeny of pRF4-injected worms exhibiting the Roller phenotype was not affected by either the single or double deletions (Figure 4A), suggesting that HPL-1 and HPL-2 are not required for array formation or transmission. To analyze de novo centromere formation, we propagated Roller worms generated by injection of a p64xLacO/pRF4 mixture into the *hpl-1(tm1624);hpl-2(tm1489)* double mutant for multiple generations and performed immunofluorescence. Arrays in the double mutant had CeCENP-A signals on opposing sides (Figure 4B), similar to arrays in wild-type worms (Figure 1C). Thus, robust de novo centromerization is observed when both *C. elegans* HP1 proteins are absent.

We next analyzed H3K9 trimethylation (H3K9me3), the modification recognized by HP1-family proteins that is representative of heterochromatin. Arrays selected over multiple generations in wild-type worms exhibited strong H3K9me3 staining (Figure S4A) [26], indicating compatibility of this heterochromatic mark with centromerization and segregation. In the *hpl-1(tm1624);hpl-2(tm1489)* double mutant, H3K9me3 staining on arrays was reduced by >90% (signal in the double mutant was $8.5\% \pm 5.7\%$ [$n = 11$] of that in controls; Figure S4A). Thus, H3K9me3 is strongly enriched on the propagated repetitive arrays in an HP1-dependent manner, but neither this accumulation nor the HP1 family proteins that bind to it are essential for de novo centromerization.

Partial Inhibition of Heterochromatin Protein 1 Accelerates Acquisition of Segregation Competence

We next analyzed the consequence of HP1-family protein inhibitions immediately after DNA injection. Inhibiting both HPL-1 and HPL-2 has pleiotropic deleterious effects; therefore, for the acute imaging assays, we analyzed single inhibitions. Array formation was not affected by inhibition of either protein by

mutation or RNAi (Figure S4B). To analyze segregation, we chose the single HPL-1 inhibition because it exhibits fewer defects compared to the HPL-2 inhibition, suggesting that it is a weak perturbation of heterochromatin.

In one-cell-stage *hpl-1(RNAi)* embryos, we observed a 6-fold increase in the frequency of segregating arrays compared to controls (Figures 4C and 4D); this is a modest effect, because only one array (from a total of ~100 arrays in 30 embryos) was observed to segregate in controls. This observed increase is not due to increased time spent in the first division or to an increased number of arrays formed following HPL-1 inhibition (data not shown). By the five- to eight-cell stage, the frequency of segregating arrays was not significantly different between HPL-1-inhibited and wild-type embryos. Thus, weak heterochromatin inhibition accelerates acquisition of segregation competence but does not affect the percentage of arrays ultimately able to segregate. We did not detect significant levels of H3K9me3 on newly formed arrays in the early divisions (Figure S4C), or even in later stage embryos, suggesting that the strong enrichment observed after propagation for multiple generations (Figure S4A) occurs on a substantially longer time scale than centromerization.

Cumulatively, the results above show that heterochromatin assembly is not required for extrachromosomal array formation or de novo centromerization in *C. elegans* embryos and suggest that weakening heterochromatin may accelerate centromerization. These conclusions contrast with the conclusions derived from studies in fission yeast and cultured *Drosophila* cells. One potential explanation for the difference in the relationship between heterochromatin and de novo centromerization between systems could be the transcriptional status of their genomes. Fission yeast and *Drosophila* cells in culture are actively transcribing their genomes and experiencing transcription-coupled histone turnover; heterochromatic regions in these cells are silenced and may therefore provide a neighborhood permissive for new CENP-A deposition. In *C. elegans*, transcription is inhibited during early embryonic divisions [27], and hence heterochromatin may not be important for CENP-A domains to form.

Conclusion

The results described here establish extrachromosomal arrays in *C. elegans* as a robust model for de novo centromerization. Arrays form soon after fertilization but take additional time to mature for autonomous segregation. Both array formation and transmission can occur in the absence of HP1 family proteins (Figure 4E). Although *C. elegans* is holocentric, it employs conserved machinery involved in CENP-A targeting and chromosome segregation [14, 28]. Thus, investigation of de novo centromerization in *C. elegans* has the potential to inform efforts on artificial chromosome engineering in human cells, especially the mechanisms that self-organize CENP-A chromatin to form a platform for kinetochore assembly. In particular, two of the attributes of extrachromosomal arrays—the robust ability to build an autonomous segregating unit independent of DNA sequence and maintain transgene expression from the introduced sequence in somatic cells—are key goals of artificial chromosome engineering for therapeutic delivery of genetic material in humans [29].

Experimental Procedures

Worm Strains, RNA Interference, and DNA Injection

C. elegans strains used in this study are listed in Table S1. All strains were maintained at 20°C, except for PFR40, PFR61, OD568, and OD569, which

were maintained at 16°C. Double-stranded RNAs (dsRNAs) were prepared as described [30] using primers containing T3 and T7 promoters and genomic DNA or cDNA as templates. RNAi was performed by soaking larval L4 worms in 5 μ l 1 μ g/ml dsRNAs (Table S2) for 24 hr in a humidified chamber and recovering soaked worms on NGM plates seeded with *E. coli* OP50 [31]. Soaked worms were recovered for 24 hr for array segregation experiments or 40 hr for array formation experiments. Purified plasmid DNA (100 ng/ μ l) was injected into gonads of young adult worms using standard methods.

Immunofluorescence

Immunofluorescence microscopy was performed as described previously [32] using a 20 min cold methanol fixation. Antibodies used against CeCENP-A, KNL-2, CeCENP-C, KNL-1, NDC-80, and BUB-1 were directly labeled with fluorescent dyes (Cy2, Cy3, or Cy5) and used at 1 μ g/ml [30, 33]. Recombinant LacI purified from *Escherichia coli* was added to the fixed embryos for 90 min and then crosslinked in 3% formaldehyde for 15 min as described [34]. Other immunofluorescence experiments were performed in a strain expressing GFP::LacI, so no recombinant LacI was added. Antibodies against LacI (mouse monoclonal; Upstate 05-503) and H3K9Me3 (rabbit polyclonal; Abcam Ab8898) were used with fluorescent-dye-conjugated secondary antibodies. Images were acquired using a 100 \times , 1.35 NA Olympus UPlanApo oil objective and a CoolSnap CCD camera (Roper Scientific) mounted on a DeltaVision deconvolution microscope system (Applied Precision). All fixed images are projections of wide-field z planes acquired every 0.2 μ m and deconvolved using Softworx software (Applied Precision).

Live Imaging

DNA-injected worms were imaged 4–8 hr after injection. Worms were anesthetized in 1 mg/ml Tricaine (ethyl 3-aminobenzoate methanesulfonate salt) and 0.1 mg/ml of tetramisole hydrochloride dissolved in M9 and were then transferred to an agarose pad for imaging as described [31]. Gonads and in utero embryos were imaged in 80 \times 0.5 μ m z series. Embryos were dissected in M9 medium and imaged on agar pads or dissected in meiosis medium and mounted on a metal holder and imaged in 9 \times 1 μ m z series at 1 min time intervals with a Yokogawa spinning-disk confocal head (CSU-X1) mounted on a Zeiss Axio Observer Z1 inverted microscope system equipped with a 63 \times 1.4 NA Plan Apochromat objective and a QuantEM:512SC EMCCD camera (Photometrics). Acquisition parameters, shutters, and focus were controlled by AxioVision software (Zeiss).

Supplemental Information

Supplemental Information includes four figures and two tables and can be found with this article online at doi:10.1016/j.cub.2011.09.016.

Acknowledgments

We thank Anne Villeneuve, in whose lab the GFP::LacI strain was generated; Diego Folco for useful discussions; and Becky Green and other members of the Oegema and Desai laboratories for comments on the manuscript. This work was supported by a grant from the National Institutes of Health to A.D. (GM074215) and a fellowship from the Croucher Foundation (Hong Kong) to K.W.Y.Y. K.O. and A.D. receive salary and additional support from the Ludwig Institute for Cancer Research.

Received: July 5, 2011

Revised: August 30, 2011

Accepted: September 7, 2011

Published online: October 20, 2011

References

- Mello, C.C., Kramer, J.M., Stinchcomb, D., and Ambros, V. (1991). Efficient gene transfer in *C. elegans*: extrachromosomal maintenance and integration of transforming sequences. *EMBO J.* 10, 3959–3970.
- Stinchcomb, D.T., Shaw, J.E., Carr, S.H., and Hirsh, D. (1985). Extrachromosomal DNA transformation of *Caenorhabditis elegans*. *Mol. Cell. Biol.* 5, 3484–3496.
- Folco, H.D., Pidoux, A.L., Urano, T., and Allshire, R.C. (2008). Heterochromatin and RNAi are required to establish CENP-A chromatin at centromeres. *Science* 319, 94–97.
- Ishii, K., Ogiyama, Y., Chikashige, Y., Soejima, S., Masuda, F., Kakuma, T., Hiraoka, Y., and Takahashi, K. (2008). Heterochromatin integrity affects chromosome reorganization after centromere dysfunction. *Science* 321, 1088–1091.
- Ketel, C., Wang, H.S., McClellan, M., Bouchonville, K., Selmecki, A., Lahav, T., Gerami-Nejad, M., and Berman, J. (2009). Neocentromeres form efficiently at multiple possible loci in *Candida albicans*. *PLoS Genet.* 5, e1000400.
- Mejia, J.E., Alazami, A., Willmott, A., Marschall, P., Levy, E., Earnshaw, W.C., and Larin, Z. (2002). Efficiency of de novo centromere formation in human artificial chromosomes. *Genomics* 79, 297–304.
- Nakashima, H., Nakano, M., Ohnishi, R., Hiraoka, Y., Kaneda, Y., Sugino, A., and Masumoto, H. (2005). Assembly of additional heterochromatin distinct from centromere-kinetochore chromatin is required for de novo formation of human artificial chromosome. *J. Cell Sci.* 118, 5885–5898.
- Williams, B.C., Murphy, T.D., Goldberg, M.L., and Karpen, G.H. (1998). Neocentromere activity of structurally acentric mini-chromosomes in *Drosophila*. *Nat. Genet.* 18, 30–37.
- Cheeseman, I.M., and Desai, A. (2008). Molecular architecture of the kinetochore-microtubule interface. *Nat. Rev. Mol. Cell Biol.* 9, 33–46.
- Santaguida, S., and Musacchio, A. (2009). The life and miracles of kinetochores. *EMBO J.* 28, 2511–2531.
- Kanda, T., Otter, M., and Wahl, G.M. (2001). Mitotic segregation of viral and cellular acentric extrachromosomal molecules by chromosome tethering. *J. Cell Sci.* 114, 49–58.
- Hubbard, E.J., and Greenstein, D. (2005). Introduction to the germ line. *WormBook*, 1–4.
- Schwarzstein, M., Wignall, S.M., and Villeneuve, A.M. (2010). Coordinating cohesion, co-orientation, and congression during meiosis: lessons from holocentric chromosomes. *Genes Dev.* 24, 219–228.
- Maddox, P.S., Hyndman, F., Monen, J., Oegema, K., and Desai, A. (2007). Functional genomics identifies a Myb domain-containing protein family required for assembly of CENP-A chromatin. *J. Cell Biol.* 176, 757–763.
- McNally, K.L., and McNally, F.J. (2005). Fertilization initiates the transition from anaphase I to metaphase II during female meiosis in *C. elegans*. *Dev. Biol.* 282, 218–230.
- Heun, P., Erhardt, S., Blower, M.D., Weiss, S., Skora, A.D., and Karpen, G.H. (2006). Mislocalization of the *Drosophila* centromere-specific histone CID promotes formation of functional ectopic kinetochores. *Dev. Cell* 10, 303–315.
- Kagansky, A., Folco, H.D., Almeida, R., Pidoux, A.L., Boukaba, A., Simmer, F., Urano, T., Hamilton, G.L., and Allshire, R.C. (2009). Synthetic heterochromatin bypasses RNAi and centromeric repeats to establish functional centromeres. *Science* 324, 1716–1719.
- Olszak, A.M., van Essen, D., Pereira, A.J., Diehl, S., Manke, T., Maiato, H., Saccani, S., and Heun, P. (2011). Heterochromatin boundaries are hotspots for de novo kinetochore formation. *Nat. Cell Biol.* 13, 799–808.
- Alonso, A., Hasson, D., Cheung, F., and Warburton, P.E. (2010). A paucity of heterochromatin at functional human neocentromeres. *Epigenetics Chromatin* 3, 6.
- Grimes, B.R., Babcock, J., Rudd, M.K., Chadwick, B., and Willard, H.F. (2004). Assembly and characterization of heterochromatin and euchromatin on human artificial chromosomes. *Genome Biol.* 5, R89.
- Nakano, M., Cardinale, S., Noskov, V.N., Gassmann, R., Vagnarelli, P., Kandels-Lewis, S., Larionov, V., Earnshaw, W.C., and Masumoto, H. (2008). Inactivation of a human kinetochore by specific targeting of chromatin modifiers. *Dev. Cell* 14, 507–522.
- Okada, T., Ohzeki, J., Nakano, M., Yoda, K., Brinkley, W.R., Larionov, V., and Masumoto, H. (2007). CENP-B controls centromere formation depending on the chromatin context. *Cell* 131, 1287–1300.
- Okamoto, Y., Nakano, M., Ohzeki, J., Larionov, V., and Masumoto, H. (2007). A minimal CENP-A core is required for nucleation and maintenance of a functional human centromere. *EMBO J.* 26, 1279–1291.
- Couteau, F., Guerry, F., Muller, F., and Palladino, F. (2002). A heterochromatin protein 1 homologue in *Caenorhabditis elegans* acts in germline and vulval development. *EMBO Rep.* 3, 235–241.
- Schott, S., Coustham, V., Simonet, T., Bedet, C., and Palladino, F. (2006). Unique and redundant functions of *C. elegans* HP1 proteins in post-embryonic development. *Dev. Biol.* 298, 176–187.
- Bean, C.J., Schaner, C.E., and Kelly, W.G. (2004). Meiotic pairing and imprinted X chromatin assembly in *Caenorhabditis elegans*. *Nat. Genet.* 36, 100–105.

27. Edgar, L.G., Wolf, N., and Wood, W.B. (1994). Early transcription in *Caenorhabditis elegans* embryos. *Development* 120, 443–451.
28. Cheeseman, I.M., Niessen, S., Anderson, S., Hyndman, F., Yates, J.R., 3rd, Oegema, K., and Desai, A. (2004). A conserved protein network controls assembly of the outer kinetochore and its ability to sustain tension. *Genes Dev.* 18, 2255–2268.
29. Macnab, S., and Whitehouse, A. (2009). Progress and prospects: human artificial chromosomes. *Gene Ther.* 16, 1180–1188.
30. Oegema, K., Desai, A., Rybina, S., Kirkham, M., and Hyman, A.A. (2001). Functional analysis of kinetochore assembly in *Caenorhabditis elegans*. *J. Cell Biol.* 153, 1209–1226.
31. Green, R.A., Kao, H.L., Audhya, A., Arur, S., Mayers, J.R., Fridolfsson, H.N., Schulman, M., Schloissnig, S., Niessen, S., Laband, K., et al. (2011). A high-resolution *C. elegans* essential gene network based on phenotypic profiling of a complex tissue. *Cell* 145, 470–482.
32. Oegema, K., Desai, A., Rybina, S., Kirkham, M., and Hyman, A.A. (2001). Functional analysis of kinetochore assembly in *Caenorhabditis elegans*. *J. Cell Biol.* 153, 1209–1226.
33. Desai, A., Rybina, S., Müller-Reichert, T., Shevchenko, A., Shevchenko, A., Hyman, A., and Oegema, K. (2003). KNL-1 directs assembly of the microtubule-binding interface of the kinetochore in *C. elegans*. *Genes Dev.* 17, 2421–2435.
34. Monen, J., Maddox, P.S., Hyndman, F., Oegema, K., and Desai, A. (2005). Differential role of CENP-A in the segregation of holocentric *C. elegans* chromosomes during meiosis and mitosis. *Nat. Cell Biol.* 7, 1248–1255.